Supplemental material

Lei et al., https://doi.org/10.1084/jem.20172359

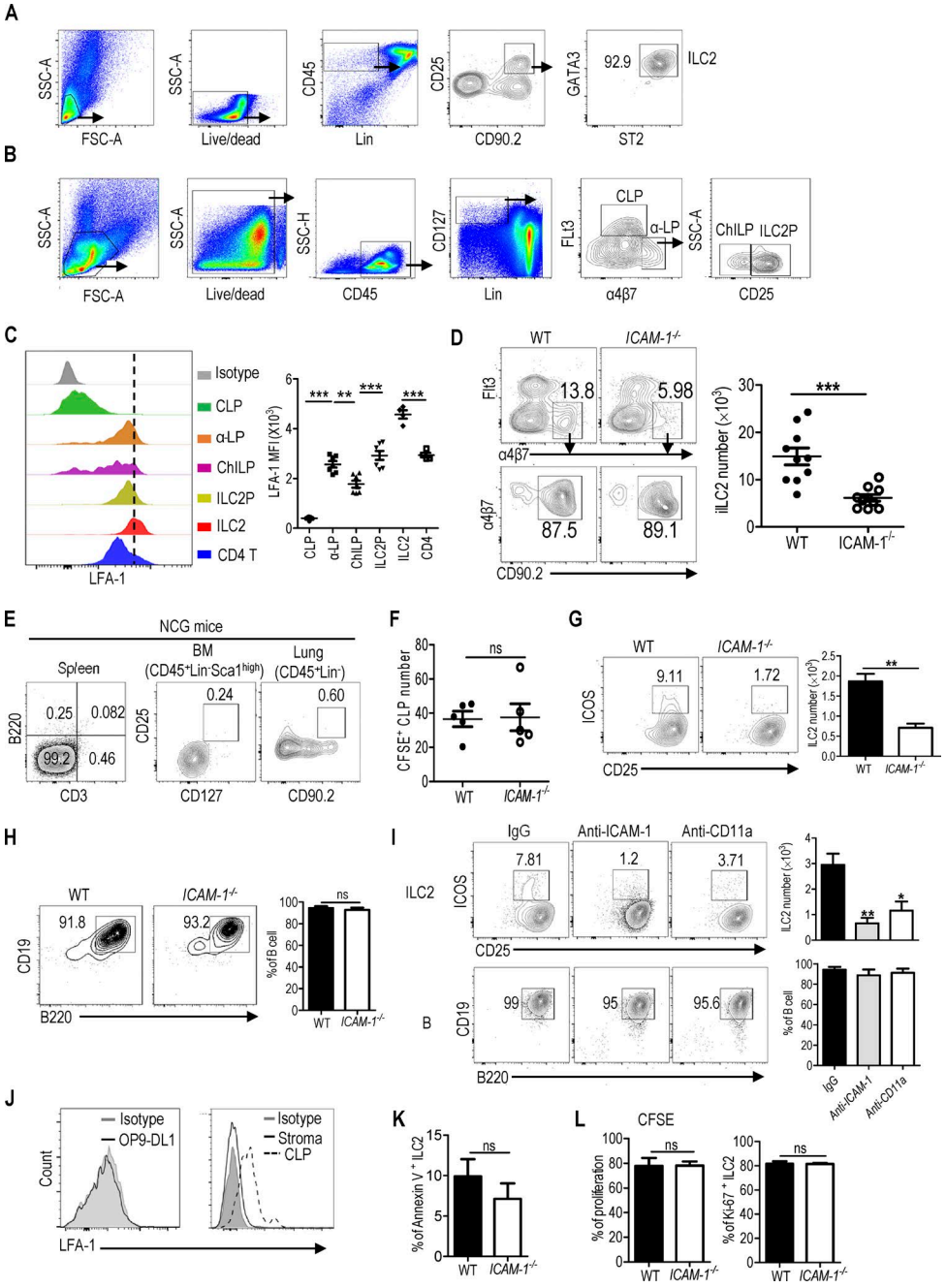

Figure S1. **ICAM-1 is required for the development of ILC2. (A)** Gating strategy of lung ILC2 ($CD45^+Lin^-CD90.2^+CD25^+GATA3^{high}ST2^+$). Data are representative results from eight mice. **(B)** Gating strategy of CLP ($CD45^+Lin^-CD127^+Flt3^+\alpha4\beta7^-$), α-LP ($CD45^+Lin^-CD127^+Flt3^-\alpha4\beta7^+$), ChILP ($CD45^+Lin^-CD127^+Flt3^-\alpha4\beta7^+CD25^-$), and ILC2P ($CD45^+Lin^-CD127^+Flt3^-\alpha4\beta7^+CD25^+$) in the BM of adult mice, pregated on live cells. Data are representative results from six mice. **(C)** Expression of LFA-1 on CLP, α-LP, ChILP, and ILC2P in BM as well as on ILC2 and $CD4^+$ T cells in lung from WT mice (n = 4–7). Light gray represents the isotype control. **(D)** Representative flow cytometry plots of BM iILC2s (pregated on $CD45^+Lin^-CD127^+$ cells) and the number of BM iILC2s from WT and *ICAM-1*$^{-/-}$ mice (n = 10 mice/group). **(E)** Representative flow cytometry plots of $B220^+$ B and $CD3^+$ T cells in spleen, and BM iILC2 and lung ILC2 from NCG mice . **(F)** WT recipient mice were lethally irradiated with 9.5 Gy and were reconstituted by intravenous injection of 10 million $CFSE^+$ BM from WT and *ICAM-1*$^{-/-}$ mice, respectively. 18 h later, the number of $CFSE^+$ CLP was evaluated by flow cytometry (n = 5 mice/group). **(G)** CLPs from WT and *ICAM-1*$^{-/-}$ mice were co-cultured with OP9-DL1 in the presence of IL-7 (10 ng/ml) for 9–10 d, and the frequencies of ILC2 (pregated on $CD45^+Lin^-$ cells) as well as ILC2 numbers were shown. **(H)** Frequencies of B cells ($CD19^+B220^+$) derived from WT and *ICAM-1*$^{-/-}$ CLPs after co-culture with OP9 cells for 10 d. **(I)** The effect of anti–ICAM-1 and anti-CD11a on the ILC2 and B cell differentiation from CLPs was shown. ILC2 differentiation from CLP was performed as in G and B cell differentiation was done as in H. **(J)** Enumeration of LFA-1 expression on OP9-DL1, BM stroma cells ($CD45^-Lin^-TER\text{-}119^-$), and CLP. Light gray represents the isotype control. **(K)** Frequencies of Annexin V^+ iILC2s in BM from WT and *ICAM-1*$^{-/-}$ mice after culture in the presence of IL-7 (10 ng/ml) and IL-33 (10 ng/ml) for 24 h. **(L)** Proliferation of iILC2s determined by CFSE staining in BM cultured as in K for 3 d (left). The right showed the frequencies of ki-67$^+$ BM iILC2s from WT and *ICAM-1*$^{-/-}$ mice after 6 d in the presence of IL-2 (10 ng/ml), IL-7 (20 ng/ml), and IL-33 (100 ng/ml). Data are representative of two (A–C, E, F and J) to three (D, G–I, K, and L) independent experiments. Error bars show mean ± SEM; *, $P < 0.05$; **, $P < 0.01$, ***, $P < 0.001$ by unpaired Student's t test. Numbers within flow plots indicate the percentages of cells gated.

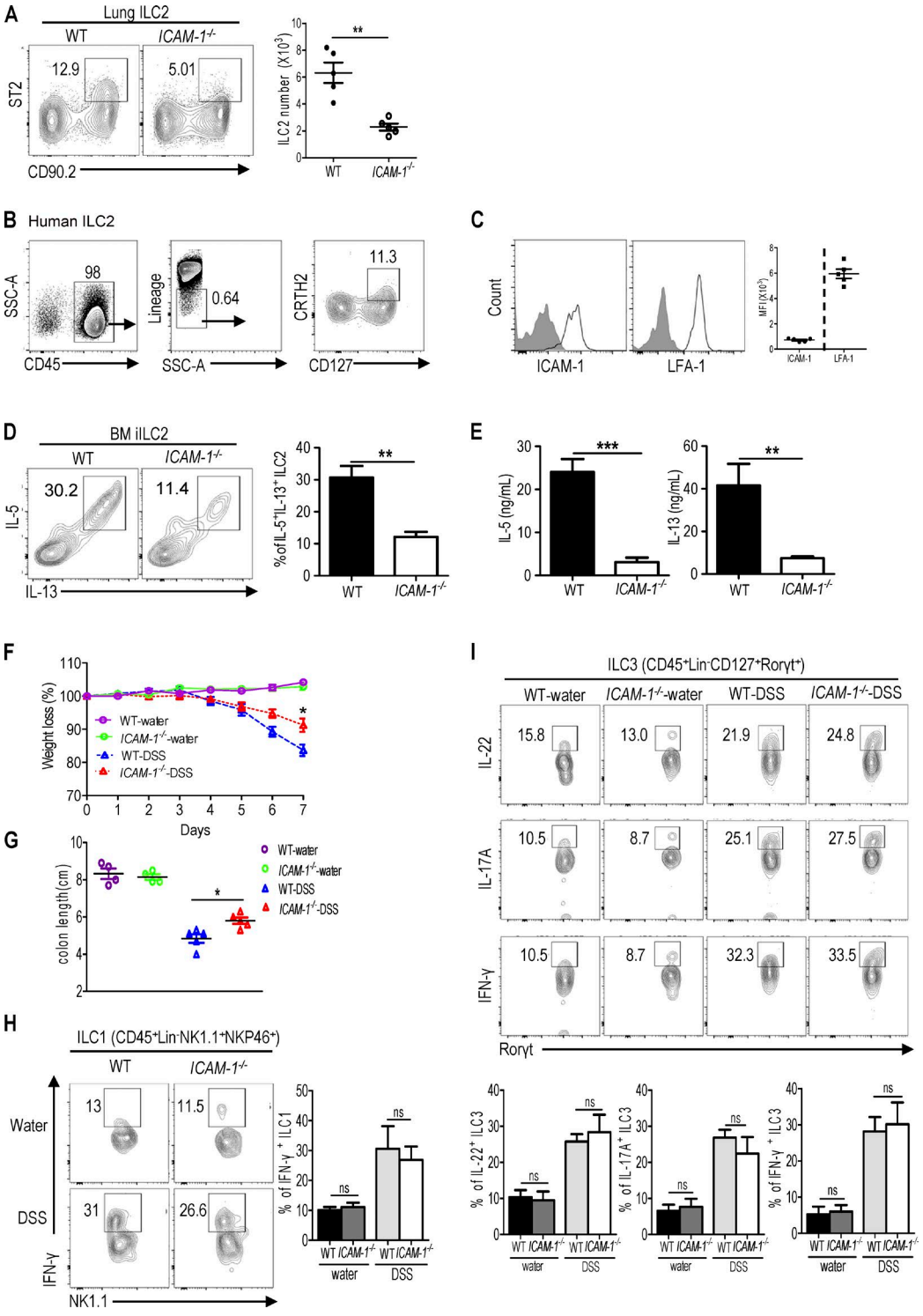

Figure S2. **ICAM-1 regulates the function of ILC2, but not ILC1 and ILC3. (A)** Flow cytometric analysis of lung ILC2 (pregated on CD45$^+$Lin$^-$ cells) from WT and *ICAM-1*$^{-/-}$ mice (n = 5 mice/group). **(B)** Representative flow cytometric analysis of human ILC2 (CD45$^+$Lin$^-$CD127$^+$CRTH2$^+$) from three independent experiments. **(C)** Flow cytometric analysis of ICAM-1 and LFA-1 expression on human ILC2s. Mean ± SEM from three independent experiments was shown on the right. MFI, mean fluorescence intensity. **(D)** Equal number of iILC2s (5,000 cells) from BM of WT and *ICAM-1*$^{-/-}$ mice were cultured for 6 d in the presence of IL-2 (10 ng/ml), IL-7 (20 ng/ml), and IL-33 (100 ng/ml). Frequencies of IL-5$^+$IL-13$^+$ iILC2s were evaluated by flow cytometry. Both representative results and mean ± SEM from three independent experiments were shown. **(E)** The amount of IL-5 and IL-13 in the culture supernatants of D was determined by ELISA. **(F–I)** WT and *ICAM-1*$^{-/-}$ mice were given normal water (n = 4 mice/group) or 2.5% DSS in drinking water (n = 5 mice/group) for 7 d. Body weight loss (F) and colon length (G) were shown. **(H)** Flow cytometric plots of the frequencies of IFN-γ$^+$ in ILC1s from colon; both representative results and mean ± SEM were shown. **(I)** Flow cytometric analysis of IL-22$^+$, IL-17A$^+$, and IFN-γ$^+$ cells in total ILC3s (CD45$^+$Lin$^-$CD127$^+$Roryt$^+$) from colon. Data are representative of two (A and F–I) to three (B–E) independent experiments. Error bars show the mean ± SEM *, P < 0.05; **, P < 0.01; ***, P < 0.001 by unpaired Student's t test. ns, not significant. Numbers within flow plots indicate the percentages of cells gated.

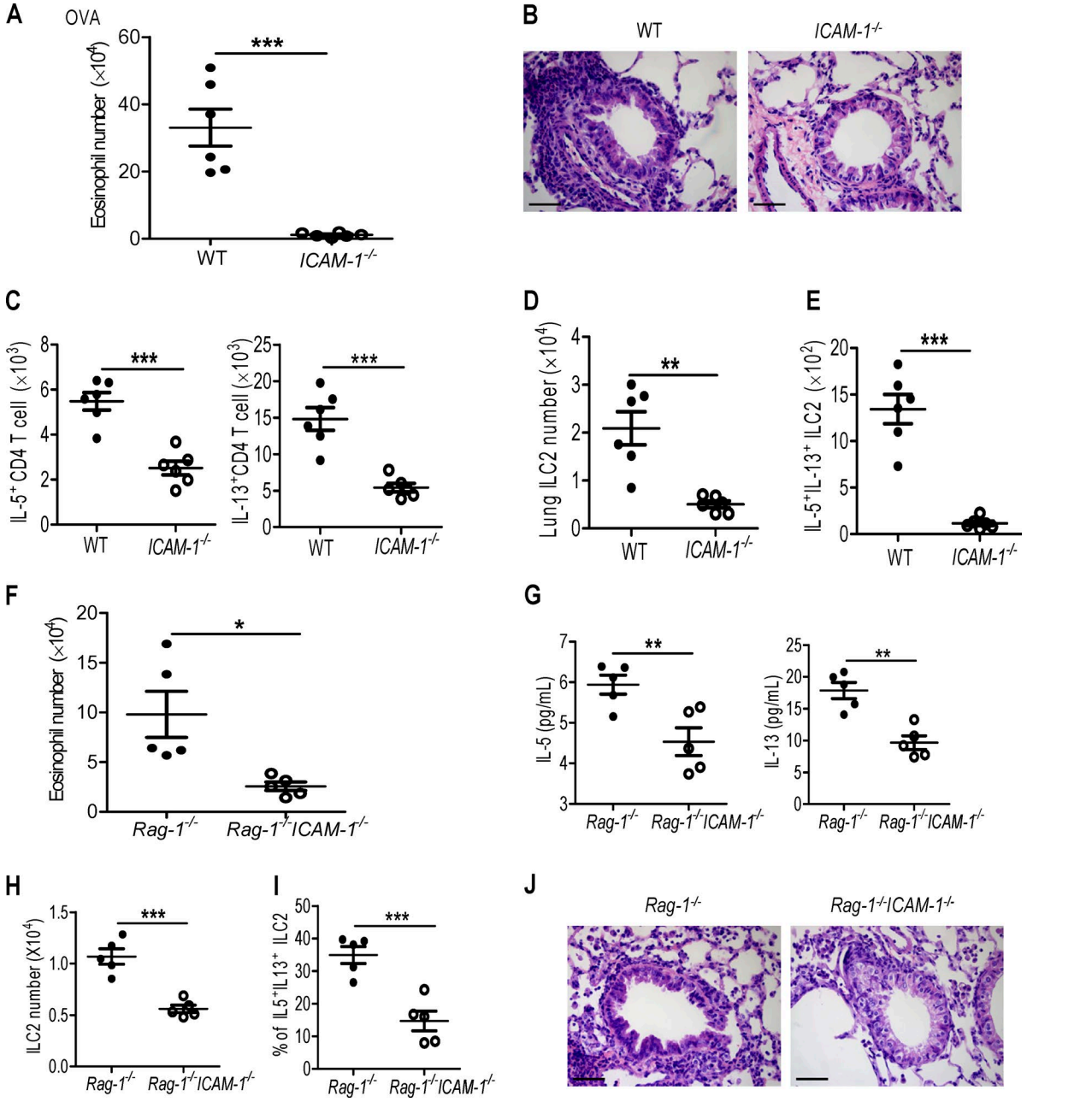

Figure S3. **Effect of ICAM-1 on ILC2-induced lung inflammation is independent of Th2 response. (A–D)** WT and *ICAM-1*$^{-/-}$ mice were sensitized with 100 µg OVA + Alum on day 0 and day 7 (n = 6 per group). On day 14, mice were intranasally challenged with 100 µg OVA for three consecutive days. Mice were sacrificed 24 h after the last challenge. **(A)** The number of eosinophils from BAL in WT and *ICAM-1*$^{-/-}$ mice is shown. **(B)** Representative H&E staining of lung sections (bars, 100 µm). **(C)** The number of IL-5^{+} CD4 T and IL-13^{+} CD4 T cells in lung is shown. **(D)** The number of ILC2 in lungs from WT and *ICAM-1*$^{-/-}$ mice after OVA treatment. **(E)** The number of IL-5^{+}IL-13^{+} ILC2s in lungs from WT and *ICAM-1*$^{-/-}$ mice. **(F–J)** *Rag*$^{-/-}$ and *Rag*$^{-/-}$*ICAM-1*$^{-/-}$ mice were intranasally challenged with papain for five consecutive days. Mice were sacrificed 24 h after the last challenge (n = 5 per group). **(F)** The number of eosinophils from lung BAL was shown. **(G)** The amount of IL-5 and IL-13 in BAL was determined by ELISA. **(H)** Lung ILC2 numbers. **(I)** Frequencies of IL-5^{+}IL-13^{+} in lung ILC2s after cell stimulation cocktail treatment for 4 h. **(J)** Representative H&E staining of lung sections. Bars, 100 µm. Data are representative of two independent experiments. Error bars show the mean ± SEM; *, P < 0.05; **, P < 0.01; ***, P < 0.001 by unpaired Student's t test.

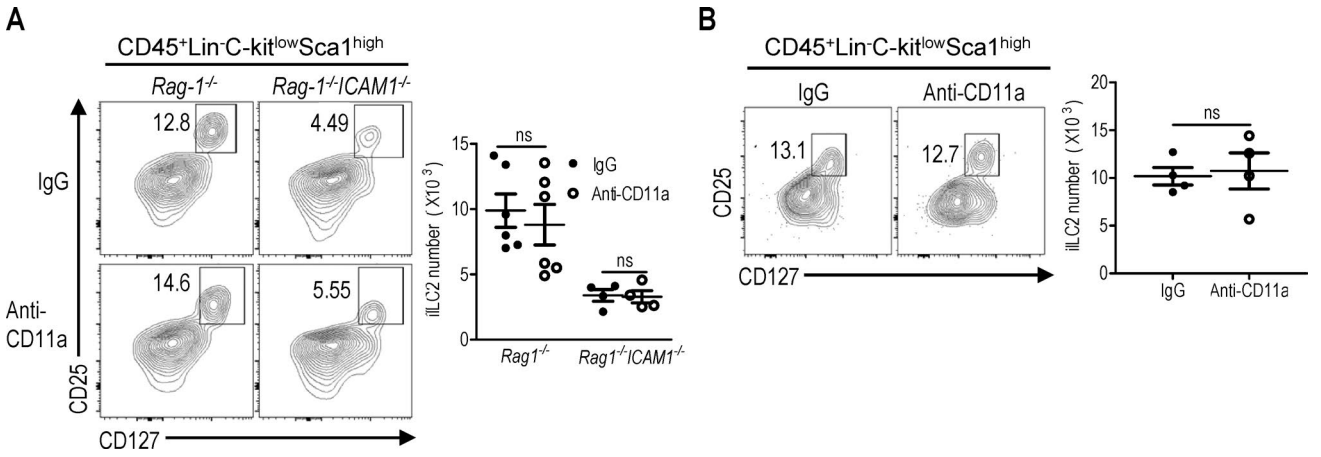

Figure S4. **Anti-CD11a does not influence the level of BM iILC2s. (A)** *Rag1*$^{-/-}$ (*n* = 6 per group) and *Rag*$^{-/-}$*ICAM-1*$^{-/-}$ (*n* = 4 per group) mice were injected intraperitoneally with anti-mouse CD11a (100 µg/mouse) or IgG (100 µg/mouse) control on day 0, followed by intranasally challenged with IL-33 (500 ng/mouse/d) for three consecutive days. Mice were sacrificed on day 4. Flow cytometric analysis of BM iILC2 (pregated on CD45^{+}Lin^{-}C-kit^{low}Sca1^{high} cells). Both representative data and mean ± SEM were included. **(B)** *Rag1*$^{-/-}$ mice (*n* = 4 per group) were injected intraperitoneally with anti-mouse CD11a (100 µg/mouse) or IgG (100 µg/mouse) control, the levels of BM iILC2 were analyzed 3 d later. Data are representative of two independent experiments. Error bars indicate the mean ± SEM. Comparison between groups was calculated by unpaired Student's *t* test. ns, not significant. Numbers within flow plots indicate the percentages of cells gated.

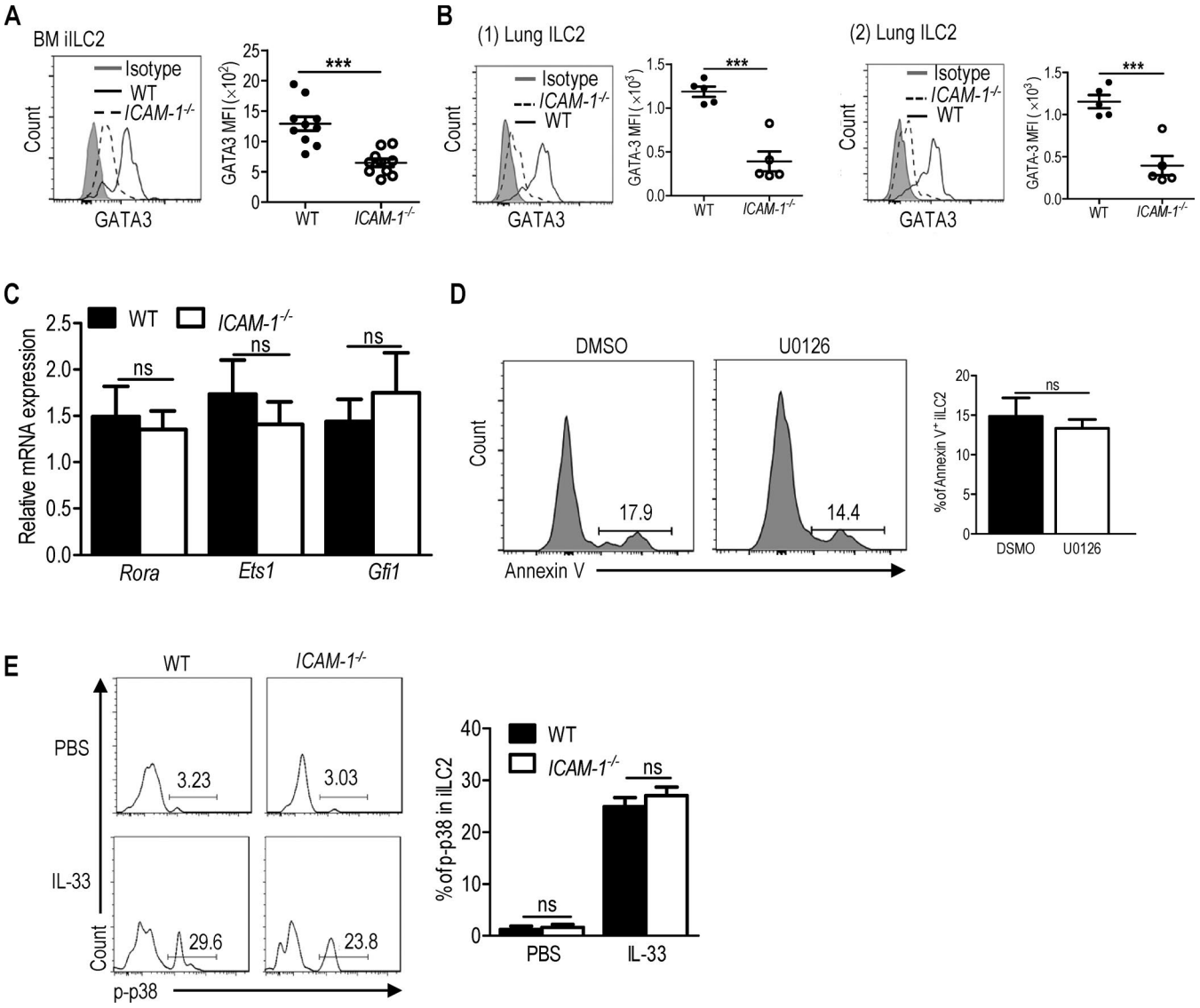

Figure S5. **ICAM-1 regulates the expression of GATA3 protein. (A)** A histogram showing the expression of GATA3 and its MFI levels in BM iILC2s ($CD45^+Lin^-CD127^+Flt3^-\alpha4\beta7^+CD90.2^+$) from WT (solid line) and *ICAM-1*$^{-/-}$ (dashed line) mice (n = 10/group). **(B)** Enumeration of GATA3 expression and its MFI levels in lung ILC2 defined as two strategies: (1) $CD45^+Lin^-CD90.2^+CD25^+$, and (2) $CD45^+Lin^-CD90.2^+ST2^+$. (n = 5 mice/group). **(C)** The expression of *Rora*, *Ets1*, and *Gfi1* in BM iILC2s from WT and *ICAM-1*$^{-/-}$ mice was analyzed by qRT-PCR. **(D)** BM from WT BM cells were cultured with DMSO or U0126 (20 µM) in the presence of IL-7 (10 ng/ml) and IL-33 (10 ng/ml) for 24 h. Percentages of Annexin V^+ iILC2s were shown. **(E)** Frequencies of p-p38 in BM iILC2s treated with PBS or IL-33 (50 ng/ml) for 30 min. Data are representative of two (B) to three (A and C–E) independent experiments. Error bars show mean ± SEM; ***, $P < 0.001$ by unpaired Student's t test. ns, not significant. Numbers within flow plots indicate the percentages of cells gated.

Table S1 shows the antibodies used in this study. Table S2 shows primer sequences used for qRT-PCR. They are included as separate Excel files.